Workspace optimization for a planar cable-suspended direct-driven robot

S. Seriani *, M. Seriani [1], P. Gallina

University of Trieste, Department of Engineering and Architecture, via A. Valerio, 10, 34127 Trieste, Italy

ARTICLE INFO

Accepted 18 January 2015

Keywords:
Repetitive Workspace Robots
Tessellation
Workspace
Cable robot
Serial robot
Industrial painting

ABSTRACT

The present work is inspired by an industrial task, i.e. spray painting a large area by means of a robotic system consisting in a Cable-Driven Parallel Robot (CDPR). In many cases, the area of the robot workspace is smaller than the area to be painted. For this reason, the base of the robot has to be shifted several times during the painting process. These robots are referred to as Repetitive Workspace Robots (RWR). In other words, in order to accomplish the whole task, they need to be moved after they have completed a sub-task locally. A cable suspended CDPR is an ideal candidate for such tasks; it can be thin, light, flexible and cost-efficient.

The question is: which is the best shape of the local workspace in these conditions? In fact, not always a larger area of the local workspace guarantees an efficient painting process. This is because the efficiency relies mainly on the shape rather than on the local workspace area itself.

In this work we employ an index [Seriani S, Gallina P, Gasparetto A, 2014] to evaluate the efficiency of the workspace of a 2-link CDPR. Finally, we show how the index value changes in relation to some geometrical parameters of the robot, thus laying the foundations for a general design methodology.

1. Introduction

In many cases, automatic or semiautomatic spray painting processes require the use of a robot which can be moved at different locations in order to accomplish the task. This is due to the area of the robot workspace, which is usually smaller than the whole area to be painted. After the robot performs the painting sub-task locally with high accuracy (fine motion) its base has to be shifted to a contiguous location (gross motion). Not always a robot with larger area workspace is preferable to a smaller area workspace. The choice depends on the workspace shape as well. In the following, a generic tool will be provided to help the designer in the evaluation of robots for these kinds of applications.

The concept of workspace is well defined in robotics. Several definitions exist. The workspace (or reachable workspace) is defined as the volume of space within which every point can be reached by the end-effector in at least one orientation. The dexterous workspace is the volume of space within which every point can be reached by the end-effector in all possible orientations, as reported for example in [1]. A controllable workspace is defined as a set of postures where forces and torques at the end-effector can be controlled [2,3]. Sometimes the workspace is analyzed in terms of manipulability [4–6] and dexterity [7].

Following a geometrical approach, Gosselin [8] defined a dynamic workspace in which the shape of the workspace depends on the accelerations of the end-effector. A survey of the basic workspace terminologies for cable-driven robots can be found in [9].

All these definitions assume that the base of the robot does not move.

For sake of simplicity let us take into account the case of planar 2D robots. In the following the term “working area” indicates the whole area that the end-effector has to cover in order to complete the technological task (e.g. a wall, or a floor). Conversely, the term “workspace”, according to the definition, specifies the planar space that the end-effector can reach without moving the robot’s base (for a planar robot for painting applications the dexterous workspace coincides with the workspace).

When a complex automated operation has to be performed by a robot on a large working area, two possible approaches exist:

1) Employing a large workspace robot; in this case its base is fixed to the reference frame.
2) Employing a small workspace robot; in this case its base has to

Abbreviations: RWR, Repetitive Workspace Robots; UECA, Uniform Expansion Covering Algorithm; CDPR, Cable-Driven Parallel Robot; AWP, Aerial Work Platform

* Corresponding author. Fax: +39 040 5583812
E-mail addresses: seriani.stefano@phd.units.it (S. Seriani), mastroser@gmail.com (M. Seriani), pgallina@units.it (P. Gallina).
[1] Present address: via Rossetti 86, 34139, Trieste, Italy.

be moved during the operation (continuously or discontinuously) in order to reach every point of the entire working area [10].

The former consists in employing a large workspace robot or a large workspace automatic device. The drawback of this approach is that, in order to reach each point of the working area, the kinematics structure needs to be stiff enough to prevent the end-effector from vibrating and bending. Therefore, usually, such robots are heavy and cumbersome. As a consequence, inertia is high and high power actuators are employed. Moreover large workspace robots are very efficient as far as the gross motion is concerned, but are less efficient in terms of fine motion. The same considerations can be applied to serial robots or large workspace cable-driven robots.

The latter approach of the two, in order to accomplish a task on a large working area, consists in moving the robot itself: the robot, not necessarily a large workspace one, can accomplish the task locally. After that, it can be moved and located, manually, automatically or semi-automatically, in a different position to accomplish a new local task; by repeating this procedure, the whole global working area can be covered efficiently.

Such a characteristic is required for example in welding applications for large structures (aircrafts, or ships).

Generally, when a robot is required to be moved with high accuracy, one or more Degrees-of-freedom (D.o.F) are “added” to the base of the robot; this, however, is not our case. A better example could be the bulldozer or the excavating machine. These are systems in which the machine operates in a set of predetermined (indexed) positions, one at a time, to dig an area that is much bigger than the local workspace. An example can be seen in [11].

Another interesting application is in painting large surfaces like a ship's flank, as visible in Fig. 1, or the façade of a house. In these cases the robot could be placed on top of a structure, e.g. an Aerial Work Platform (AWP) and moved along the surface, then, with the platform holding its position, the robot could paint the surface contained locally in its workspace.

In these setups, the part of the system in charge of the gross motion (the bulldozer driving system in the former case, the AWP in the latter) cannot, at times, be moved synchronously with the robot on top.

In the following, such robots are referred to as Repetitive Workspace Robots (RWR).

Unconventional modes of operation like that of a RWR may have specific requirements, as that of flexibility, lightness or even portability. A planar cable-suspended robot or Cable Driven Parallel Robot (CDPR) is, in our opinion, an ideal candidate for such tasks. Indeed, it is light and safe to manage, which make it flexible and portable. This means that it could be considerably easier to handle, while coupled with an AWP or similar mechanism.

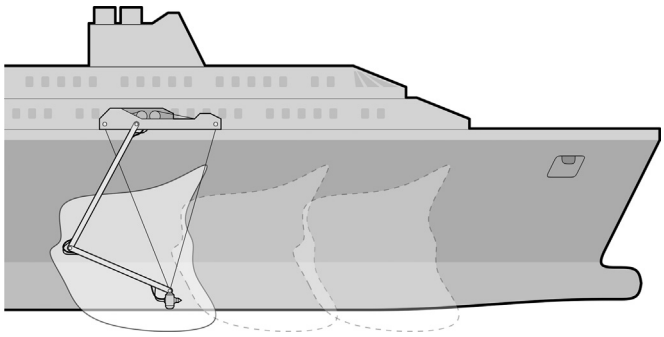

Fig. 1. An example of the spray-painting process of the side of a ship with a cable-suspended RWR. The chassis of the robot is placed at regular intervals on the length of the ship and each time it paints the wall contained in its local workspace.

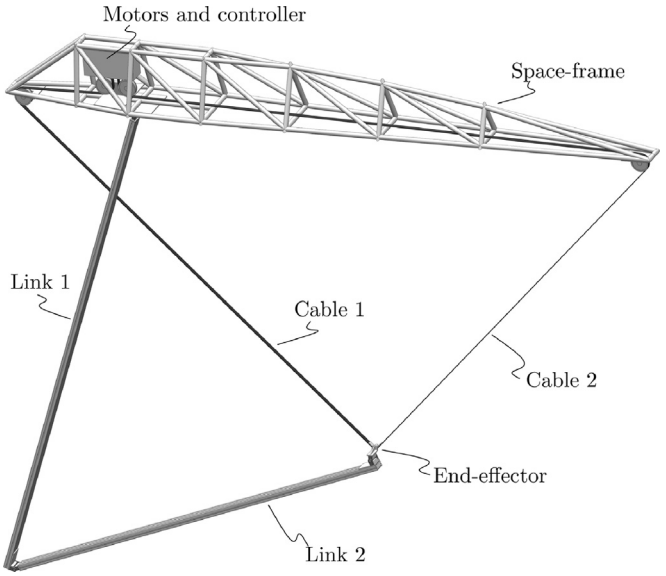

Fig. 2. The CDPR robot equipped with a 2-link passive serial manipulator. The space-frame structure at the top provides support for the cable pulleys (upper-right and left) and for the first link, near the center. It also hosts the motors, winches and controllers for the cable maneuvering.

Additionally, it can have a very large workspace area compared to its cost. Finally, being lightweight, it could be made be very efficient.

In this specific case, we couple, with the cables, a 2-link passive serial manipulator to stabilize the end-effector. This is necessary since planar cable robots tend to be labile in the direction orthogonal to the nominal workspace plane.

Following the approach of [10], we use the simple Uniform Expansion Covering Algorithm (UECA) to compute the index I_{RWR}, which will be formally described in Section 2.2. The index is then employed to optimize the geometry of a CDPR provided with a 2-link serial passive manipulator. An illustration of the robot is shown in Fig. 2, whereas the actual diagram of the model used to describe the robot’s behavior is shown in Fig. 8. We choose to calculate the index following the UECA methodology, since, contrary to the other methodologies presented in the cited paper (CIECA, GCA), this works best where the robot’s workspace has a fixed orientation. In the specific case at hand, where a CDPR is considered, the rotation of the workspace is not trivial. In fact, the robot’s kinematics is dependent on the gravity acceleration versor, therefore rendering the computation complex were the workspace shape to rotate. Additionally, this method allows for very fast computation time, more than 4 times CIECA and almost 500 times GCA.

The paper is organized as follows: in Section 2, the formulation of the I_{RWR} index is shown according to the state-of-the-art; in Section 3 the index is used as a parameter to guide the kinematics design of a cable robot; eventually, conclusions stress the importance of the index with respect to the typical definition of workspace for a RWR.

2. Methods

In this section we analyze the tessellation problem associated to RWRs, give a brief formal definition of the I_{RWR} index and illustrate how UECA is employed to compute the index from the workspace geometry.

2.1. Tessellation problem

In regards to a 2D problem, we can define the tessellation as the process of creating a plane through the repetition of a single geometric shape, resulting in the absence of overlaps and gaps.

When a planar robot is required to cover a working area larger than the workspace of the robot itself, the surface has to be partitioned, and the robot moved to cover each partition one at a time. For example: being the workspace a square, the working area should be broken in a series of juxtaposed squares, resulting in a grid-like pattern. In general, if the shape of the workspace allows for a perfect tessellation of the working area, there would be no overlapping, and thus the "efficiency" of the partitioning would be the maximum possible. This condition can be proven true for simple Cartesian robots which have a rectangular workspace. More commonly, the workspace of the robot is characterized by a specific shape which can be strongly irregular. This is the case for anthropomorphous robots, cable robots, etc. It is, at this point, easy to understand that the "efficiency" parameter should be linked to the degree of tessellation that the robot's workspace is capable to provide. In other words, efficiency is higher if the workspace produces less overlapping during the tessellation of the working area. No workspace overlapping, in practice, means that each point of the robot workspace is exploited.

In Fig. 3 we can see an example of this concept; it is immediately apparent that the working area is perfectly tessellated in the case where a square workspace is used. Indeed, in this case no overlaps are present, so the "efficiency" parameter could be thought of as the maximum possible.

What is immediately apparent from the same figure is that, for the same number of repetitions, six in this case, the tessellation with a square workspace (Fig. 3b) covers a much larger area than the one with a round workspace (c). Indeed, the left-out area is considerably larger in the case of the circular workspace. From these considerations we can infer that the circular workspace has a lower tessellation efficiency compared to the square one.

From the considerations made up to this point, being able to formally define an index linked to this notion of efficiency seems appropriate.

2.2. Formal definition and computation methodology

In this section the I_{RWR} index is defined, and the simple UECA algorithm is briefly summarized. Please refer to the previous work of Seriani [10] for an in-depth view on UECA and its performance.

Referring to Fig. 4, let A be the workspace of the robot. We can then simultaneously shift the area A in the directions NE, SE, SW, NW, according to the geographical notation, by a combination of $\pm\Delta s$ in the x and y directions together. We can define the quantity $\Delta s = \Delta x = \Delta y$, as shown in the figure.

This method applies in the same way for a generic work-space shape and not only for the case of the circle, which is merely an example to better understand how the algorithm operates.

With the aid of the contents of the same figure it is then possible to define the expanded area as

$$\begin{aligned} A_{exp} &= A_{exp}(\Delta s) \\ &= A_{NE} \cup A_{SE} \cup A_{SW} \cup A_{NW} \\ &= \tilde{A}(\Delta x, \Delta y) \cup \tilde{A}(\Delta x, -\Delta y) \cup \tilde{A}(-\Delta x, -\Delta y) \cup \tilde{A}(-\Delta x, \Delta y) \\ &= \tilde{A}(\Delta s, \Delta s) \cup \tilde{A}(\Delta s, -\Delta s) \cup \tilde{A}(-\Delta s, -\Delta s) \cup \tilde{A}(-\Delta s, \Delta s) \end{aligned} \quad (1)$$

Note that $\tilde{A}$ is the workspace A after the general translation, as shown in Fig. 4b.

In Fig. 4c it is possible to introduce the criterion for the maximum expansion. From the definition of tessellation, we define this criterion as the maximum translation which results in an expanded area A_{exp} which is still a connected space. In addition, the same area should have a single connected boundary, which translates in the condition that no gaps are present in the connected domain. It is indeed apparent that in Fig. 4c A_{exp} cannot expand further, since this would produce a gap at the center.

Note that, if the single-boundary condition is fulfilled, the space A_{exp} is necessarily connected. This is illustrated in Fig. 5.

We can finally define the Index for Repetitive Workspace Robots as the following:

$$I_{RWR} = \max(\Lambda), \quad (2)$$

where

$$\Lambda(\Delta s) = \begin{cases} \dfrac{A_{exp}(\Delta s)}{4A}, & \text{if } A_{exp} \text{ has only one boundary} \\ 0, & \text{if } A_{exp} \text{ has more than one boundary} \end{cases} \quad (3)$$

Note that A_{exp} is divided by 4 to normalize the index in the 0–1 interval.

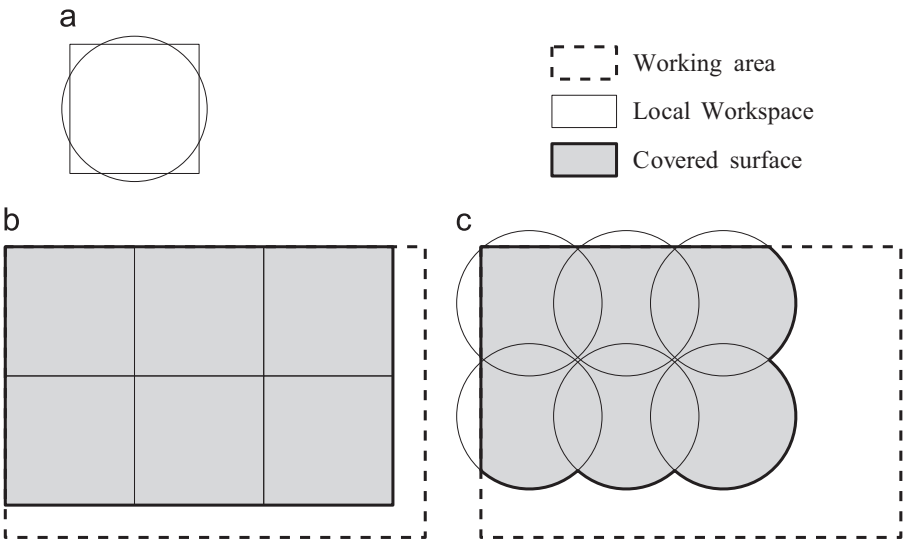

Fig. 3. Efficiency of the tessellation (in gray) of the working area (dashed line). In (a) a square and a round workspace are shown; these have the same area. In (b) one can see a partial tessellation of the working area resulting from the use of the square workspace, whereas in (c) the same is visible in case the circular one is employed.

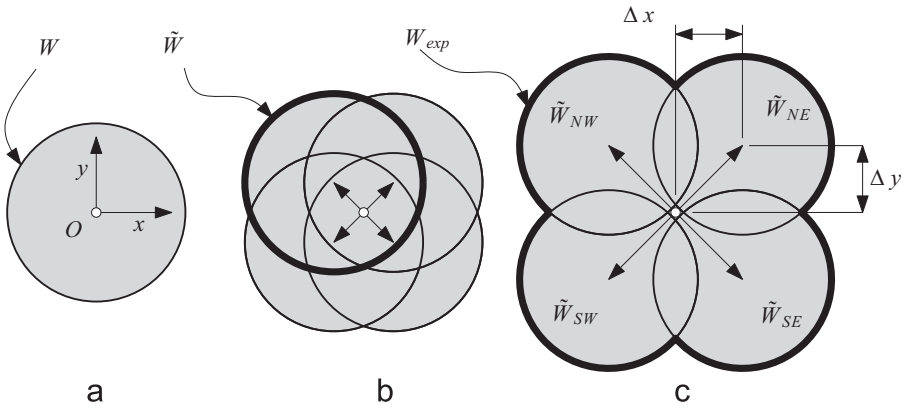

Fig. 4. Translation of the original workspace and expansion of the union of the resulting areas. The arrows show the translation of the $\tilde{A}$ areas. The gray area shows the expanded area A_{exp}. (a) shows the robot workspace, (b) illustrates a general translation step, and (c) shows the presence of a gap at the center of the frame; this is representative of the criterion for the maximum translation (expansion) of the surface.

2.3. Examples

Using the I_{RWR} index definition we propose some examples to provide a first quantitative insight. If the workspaces in Fig. 6 are considered, one can calculate the index associated to each domain. It is to be expected that the index related to the square domain in (b) will be considerably higher than one related to the circular one in (a). Also, given the definition of the index itself, such index should be equal to one, since a square shape provides the maximum tessellation efficiency.

Indeed, if Fig. 7 is considered, it is clear that these assumptions are correct. In the same figure the trend of the quantity $\Lambda(\Delta s)$ is shown for the three workspaces, and the spikes show the related I_{RWR} value. In fact, $I_{RWR} = 1$ for the square workspace (b), while $I_{RWR} \cong 0.8$ for the circular one (a). As a last consideration, one can appreciate the shallowness of the index for an anthropomorphous robot. For the workspace in Fig. 6c, we have $I_{RWR} \cong 0.6$.

3. Application of the index to the cable robot

3.1. Generic description of a CDPR robot

In this section we present the two link CDPR passive serial manipulator [12,13] which is visible in Fig. 2. It is set up by two links, two cables and two pulleys driven by two actuators and operates on a vertical plane. The 2-link serial robot is anchored on a lightweight chassis which hosts the cable pulleys as well as possible controller modules. The entire structure is lightweight and compact when stored and can be easily mounted on an external movable structure as an AWP.

The end-effector is supported by the cables and its position E on the workspace is a function of the cables angular positions ψ_1 and ψ_2. In order to avoid movements along the direction normal to the workspace plane, the end-effector is connected to the free end of a passive two-link planar two degrees-of-freedom serial manipulator by means of a revolute joint. The serial manipulator is attached to the frame in a selected point R.

The CDPR's geometrical parameters and its kinematics scheme are shown in Fig. 8.

Finally we note that the variation of the geometrical and physical parameters of this robot produces workspaces which are consistently different in shape and dimensions one from the other.

3.2. Kinematics analysis

Referring to Fig. 8, φ_1 and φ_2 are the angular orientations of the RC and CE links respectively; ψ_1 and ψ_2, the angular orientations of the A_1E and A_2E cables; l_1 and l_2, the RC and CE link lengths; (x_R, y_R), (x_E, y_E), (x_{A_1}, y_{A_1}), (x_{A_2}, y_{A_2}), the coordinates of points R, E, A_1 and A_2.

Given the position E. of the end-effector, the inverse kinematics analysis allows to calculate φ_1 and φ_2.

The virtual vector $\overrightarrow{l_t}$ is given by

$$\varphi_t = \text{atan2}\big((x_E, y_E), (x_R, y_R)\big), \tag{4}$$

$$l_t = \sqrt{(x_R - x_E)^2 + (y_R - y_E)^2} \tag{5}$$

The angular positions of the links are

$$\begin{aligned} \varphi_1 &= \varphi_t + \pi - \beta, \\ \varphi_2 &= \varphi_t + \pi + \alpha \end{aligned} \tag{6}$$

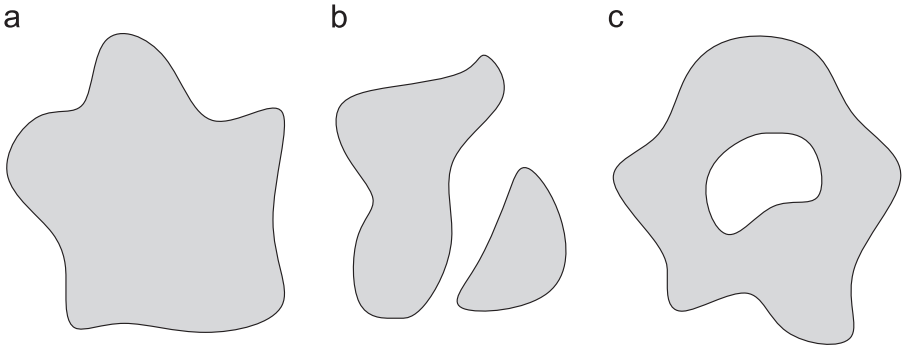

Fig. 5. Three general types of domains are presented. (a) shows a connected and gap-free space, (b) a gap-free but not connected domain, and (c) shows a connected space with a gap. Note that in (b) and (c) more than one boundary is present, while in (a) there is a single one.

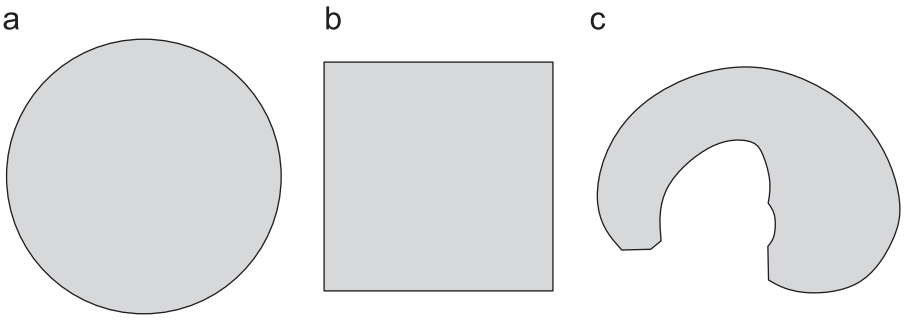

Fig. 6. Different workspace shapes. (a) and (b) are ideal geometric regular shapes, (c) is the lateral workspace of a common anthropomorphic 6 DOF robot.

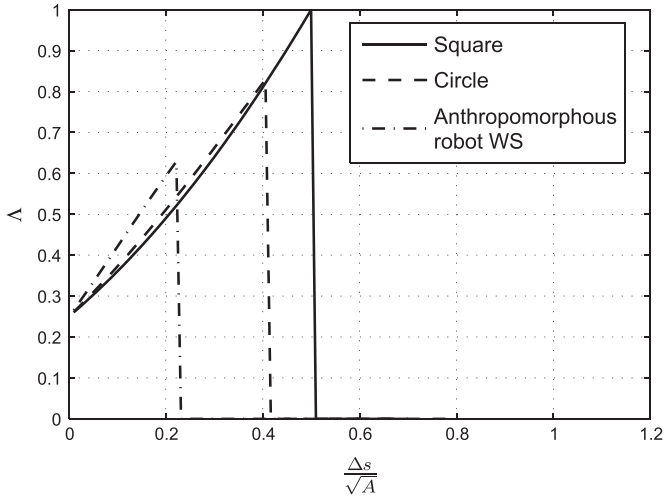

Fig. 7. Behavior of the $\Lambda(\Delta s)$ value for different workspace shapes, related to the normalized displacement $\Delta s/\sqrt{A}$, where A is the workspace area. The maximum value for each curve is the I_{RWR} index of the related workspace. The shapes used are visible in Fig. 6.

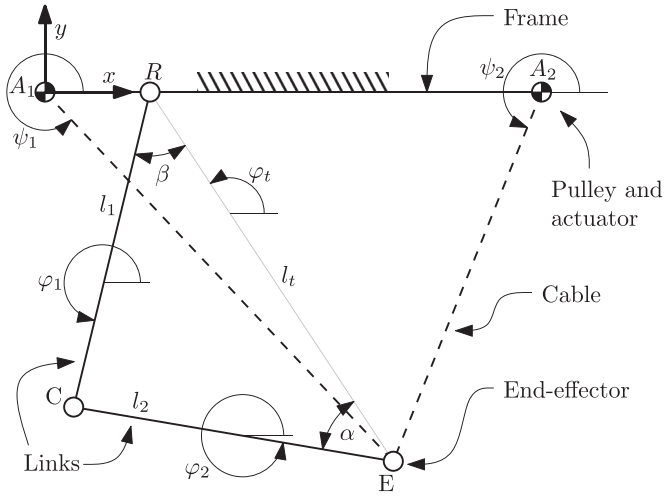

Fig. 8. Two-links CDPR passive serial manipulator.

where

$$\alpha = \operatorname{acos}\left(\frac{l_2^2 + l_t^2 - l_1^2}{2 l_2 l_t}\right),$$
$$\beta = \operatorname{acos}\left(\frac{l_1^2 + l_t^2 - l_2^2}{2 l_1 l_t}\right). \tag{7}$$

Furthermore, we can define the ratio between the length of the two links l_1 and l_2,

$$\xi = \frac{l_1}{l_2}. \tag{8}$$

3.3. Workspace definition

The workspace A of the two links CDPR passive serial manipulator is defined as the subset of space where the tensions on cables are both non-negative. The workspace A depends on the geometrical parameters of the robot (weight of the links and of the end-effector, motor positions, etc.).

Expanding further, it is possible to define the following relation for the workspace:

$$W = \{E \in \mathbb{R} | T_1 > 0 \wedge T_2 > 0\}, \tag{9}$$

where T_1 and T_2 are the cable tensions. These are obtained by means of the Newton's method, as follows:

$$X = M^{-1}B, \tag{10}$$

where the matrix M is

$$M = \begin{Bmatrix} 1 & -1 & 0 & 0 & 0 & 0 \\ 0 & -\cos(\varphi_1) & 0 & \sin(\varphi_1) & 0 & 0 \\ 0 & 1 & -1 & 0 & 0 & 0 \\ 0 & 0 & -\cos(\varphi_2) & \sin(\varphi_2) & 0 & 0 \\ 0 & 0 & 1 & 0 & \sin(\psi_1+\pi) & \sin(\psi_2+\pi) \\ 0 & 0 & 0 & 1 & \cos(\psi_1+\pi) & \cos(\psi_2+\pi) \end{Bmatrix}, \tag{11}$$

and X and B are

$$X = \begin{Bmatrix} V_R \\ V_C \\ V_E \\ H \\ T_1 \\ T_2 \end{Bmatrix}, \quad B = \begin{Bmatrix} P_1 \\ \frac{1}{2}P_1 \cos\varphi_1 \\ P_2 \\ \frac{1}{2}P_2 \cos\varphi_2 \\ P_E \\ 0 \end{Bmatrix}. \tag{12}$$

Note that V_C and V_E are the vertical forces acting on nodes C and E. H is the internal horizontal force acting on the end-effector and on the nodes. P_1, P_2 and P_E are respectively the weights of the links and of the end-effector.

3.4. Computation of the index I_{RWR} varying the ξ and x_R parameters

Having defined the kinematics and geometrical configuration of a two link CDPR passive serial manipulator, we can easily calculate the workspace W for different sets of design parameters. Specifically, we note that two parameters, among others, greatly

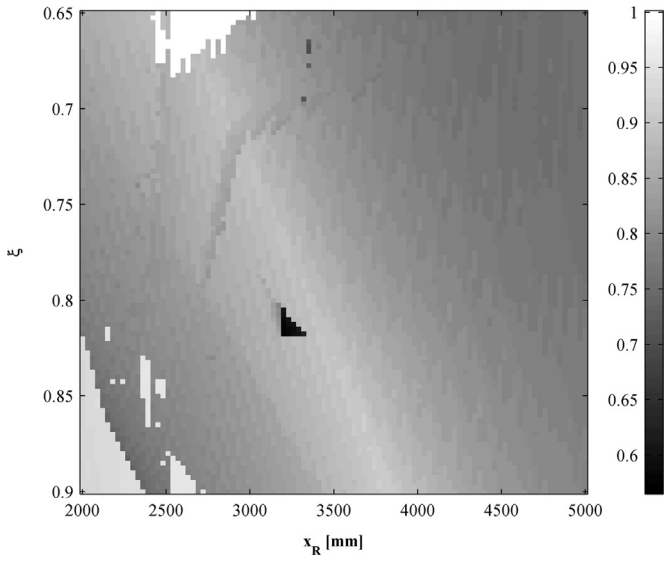

Fig. 9. Surface resulting from the values of I_{RWR} obtained by varying the x_R and ξ parameters.

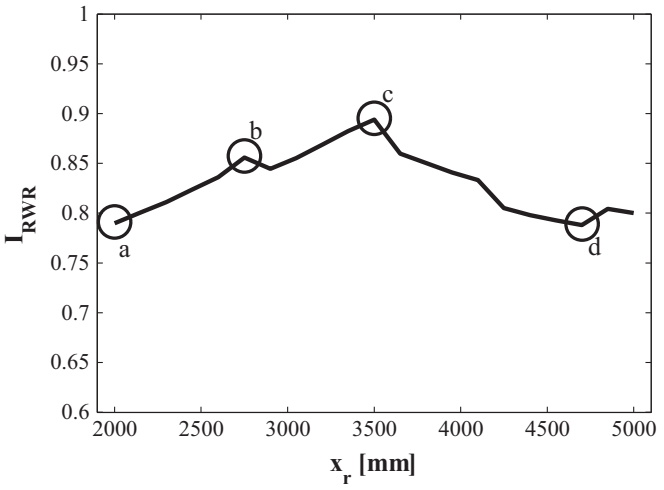

Fig. 10. In this figure the I_{RWR} indexes of the configurations obtained varying x_R from 2000 to 5000 mm are shown. The letters *a*, *b*, *c*, *d*, indicate the cases represented in detail in Fig. 11.

influence the shape of the workspace. These are the horizontal coordinate x_R of the robot node *R*, and the ratio between the length of the links, ξ. To define the actual length of the links, we fixate the sum of their lengths, thus having $l_{tot} = l_1 + l_2$. This constraint allows us to vary the geometrical configuration of the links without substantial implications on the bulk and overall weight of the robot. Moreover, we are able to perform this by acting on only one parameter, ξ.

We discretize the variation span of the two parameters, thus creating a grid. By computing the workspace for each grid-point we are able to calculate the associated I_{RWR} index for the workspaces. These are shown as a surface in Fig. 9.

The x_R parameter varies between 2000 and 5000 mm, whereas the variation interval of ξ is 0.65–0.9. The total length of the links is l_{tot}=9899 mm. All other parameters are fixed: x_B=7000 mm, x_A =0 mm, $y_{A_1} = y_{A_2} = y_R = 0$ mm, $P_1 = P_2 = 12$ kg, $P_E = 10$ kg. The end-effector (point $_E$) represents a spray gun (*WAGNER Colora GA 4000ACIC*) which bulk dimensions are $129 \times 47 \times 60$ mm^3, and weight is 0.678 kg. The spray stroke can vary from approximately 20 to 300 mm in diameter.

From the surface in the figure we can see that the index varies substantially in function of the parameters x_R and ξ. A general trend is evident in the form of a curved ridge where the points with the highest index lay. This shows a possible correlation between the considered parameters, although this is not investigated further in the present paper. Finally, we note that in the proximity of the bottom-left and upper corners of the surface, a series of white areas are present. These are errors of the UECA algorithm, which have been explained in the original paper [10] where the algorithm was first described. Furthermore, we note that near the center of the surface, a dark-gray spot is present. This is due to the formation, at those coordinates, of some irregular structures along the edge of the workspace; these contribute to a substantial decrease in the local index value.

3.5. Computation of the Index I_{RWR} varying the x_R parameter alone

The coordinate x_R (the anchor point *R* of the first link (link *RC*), as seen in Fig. 8), plays a key role in the definition of the workspace shape. The x_R variable is chosen as the optimization parameter because, as previously noted in Section 3.4, the position of joint $_R$ on the frame is strongly influential on the resulting workspace shape for this type of robot (and therefore for its I_{RWR} index). Furthermore, this parameter is easily customizable on a robot, contrary to the length of the links (which gives the ξ ratio). Nevertheless, the variation of the I_{RWR} index can be studied for any other parameter (for example ξ, l_1, l_2, the weight of the links, etc.).

Therefore, it is interesting to calculate I_{RWR} index for different values of the coordinate x_R. This way, according to the index, it is possible to select the value of x_R which guarantees that the workspace associated with the robot provides the maximum possible tessellation efficiency.

Results are presented in Figs. 10 and 11. In particular Fig. 10 shows the I_{RWR} index values obtained with a continuous variation of x_R; instead Fig. 11 allows the reader to understand the shape of the workspace for four significant x_R values, which are identified in Fig. 10 with the letters *a*, *b*, *c* and *d*.

The physical parameters of the robot are the same as those shown in Section 3.4, with the exception of the length of the links, which is now fixed by having $\xi = 0.78$.

The table in Fig. 11 shows that configuration "*c*" ($x_R = 3500$ mm) delivers the best I_{RWR} index, and therefore the best tessellation efficiency. One can well appreciate this, noting that the intersection area (shown in the 5th column) in this case is significantly smaller than in the other cases. It can therefore be inferred that the best geometrical configuration, in terms of "efficient tessellation" of a large working area, is obtained when $x_R = 3500$ mm. For the same reason the workspace produced by configuration "*d*" ($x_R = 4700$ mm) has a poor efficiency, which is immediately apparent from the large intersection area. This is consistent with the related I_{RWR} index.

In general the index I_{RWR} is shown to vary against some of its parameters. As can be seen from Fig. 9 the index is considerably more sensitive to the x_R parameter, than to the ξ parameter; in fact, once a specific ξ is selected from the map in the figure, the x_R can used efficiently to locate the maximum index value, as Figs. 10 and 11 demonstrate.

4. Conclusion

Not always a robot with a large workspace is suited to accomplish a task on a large working area. This is the case for Repetitive Workspace Robots. For this reason, we analyze a recently described index, I_{RWR}. This index was introduced as a means to evaluate the topological tessellation efficiency of these robots.

In the present work we employ this index to lay down a design

Rif.	x_R $[mm]$	Geometrical Configuration	Workspace (*Area* in pixels)	Maximum intersection WS	I_{RWR}
a	2000	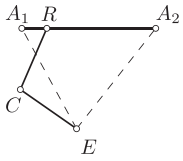	 $Area = 3823$	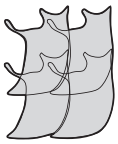	0.7911
b	2750	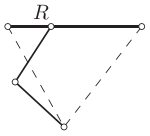	 $Area = 4474$	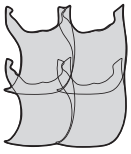	0.8571
c	3500	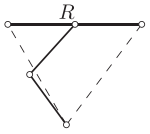	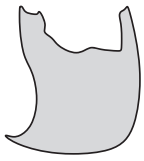 $Area = 5175$	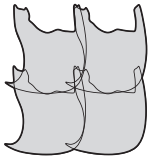	0.8950
d	4700	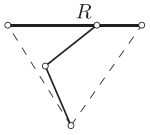	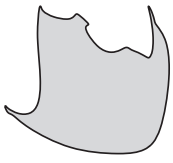 $Area = 6212$	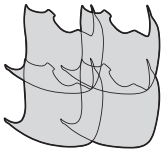	0.7889

Fig. 11. In this figure some different configurations in terms of values of the serial manipulator anchor point x_R, noted by the letters *a*, *b*, *c*, *d*, are chosen from the plot in Fig. 10 and the I_{RWR} index of the resulting workspace is shown. All other parameters are fixed: $l_{tot} = 9899$ $\xi = 0.78$, $x_B = 7000$ mm, $x_A = y_A = y_B = y_R = 0$ mm. The area (in pixels) of the resulting workspace is shown for each configuration.

methodology for a specific type of RWR, where the index is used as the main design parameter for a CDPR robot. A specific type of algorithm, the Uniform Expansion Covering Algorithm (UECA), is employed, being it well suited to cope with this type of robot. Variations in the resulting I_{RWR} values for the robot are shown in relation to variations in some of its geometrical design parameters. Finally, we show how the index can be directly used to choose a design configuration for this type of robots.

We note that this index can easily be coupled to a variety of other indexes or parameters (manipulability, dexterity, etc.).

For example, as far as CDPRs are concerned, it can be combined with indexes which take into account the tension factor values so as to generate a workspace with optimized performance [14]. Nevertheless, this work confirms preceding studies on the index' field of application, and illustrates a practical result.

References

[1] L.W. Tsai, Robot Analysis: The Mechanics of Serial and Parallel Manipulators, John Wiley and Sons, New York, NY, USA, 1999.

[2] R. Verhoeven, M. Hiller, S. Tadokoro, Workspace of tendon-driven Stewart platforms: Basics, classification, details on the planar 2-dof class, in: Proceedings of the International Conference on Motion and Vibration Control MOVIC, vol. 3, 1998, pp. 871–876.

[3] S. Tadokoro, T. Matsushima, Y. Murao, H. Kohkawa, M. Hiller, A parallel cable-driven motion base for virtual acceleration, in: Proceedings of IEEE/RSJ International Conference on Intelligent Robots and systems, Maui, Hawaii, vol. 3, 2001, pp. 1700–1705.

[4] P. Gallina, G. Rosati, Manipulability of a planar wire driven haptic device, Mech. Mach. Theory 37 (2002) 215–228.

[5] I. Dulębe, I. Karcz-Dulęba, Planning motion of manipulators with local manipulability optimization, Lect. Notes Control Inf. Sci. 422 (2012) 365–375.

[6] T. Watanabe, Effect of torque–velocity relationship on manipulability for robot manipulators, J. Mech. Robotics 3 (2011) 041007.

[7] A. Bahrami, M. Nikkhah-Bahrami, Multi-objective design of spatial cable robots, in: Proceedings of the 2nd IASTED International Conference on Robotics, Robo, 2011, pp. 345–352.

[8] C.M. Gosselin, G. Barrette, Kinematic analysis of planar parallel mechanisms actuated with cables. in: Proceedings of Symposium on Mechanisms, Machines and Mechatronics, Quebec, Canada, 2001, pp. 41–42.

[9] P. Bosscher, I. Ebert-Uphoff, Wrench-based analysis of cable-driven robots, in: Proceedings of IEEE Conference on Robotics and Automation, New Orleans, LA, 2004, pp. 4950–4955.

[10] S. Seriani, P. Gallina, A.A. Gasparetto, Performance index for planar repetitive workspace robots, J. Mech. Robotics 6 (2014) 031005.

[11] A. Papachristou, H. Valsamos, A. Dentsoras, Optimal initial positioning of excavators in digging processes, Proc. Inst. Mech. Eng. Part I: J. Syst. Control Eng. 224 (2010) 835–844.

[12] A. Trevisani, P. Gallina, R.L. Williams, Cable-direct-driven robot (CDDR) with passive SCARA support: theory and simulation, J. Intell. Robot Syst. 46 (2006) 73–94.

[13] A. Trevisani, Underconstrained planar cable-direct-driven robots: a trajectory planning, Mechatronics 20 (2010) 113–127.

[14] C.B. Phama, S.H. Yeob, G. Yangc, I.M. Chen, Workspace analysis of fully restrained cable-driven manipulators, Robotics Auton. Syst. 57 (2009) 901–912.